RAA 2018 Vol. **18** No. **5**, 58(8pp) doi: 10.1088/1674–4527/18/5/58

http://www.raa-journal.org *http://iopscience.iop.org/raa*

***R**esearch in*
***A**stronomy and*
***A**strophysics*

Hydrogen and helium shell burning during white dwarf accretion

Xiao Cui[1,2,3], Xiang-Cun Meng[1,2] and Zhan-Wen Han[1,2]

[1] Yunnan Observatories, Chinese Academy of Sciences, Kunming 650216, China; *cx@ynao.ac.cn, zhanwenhan@ynao.ac.cn*

[2] Key Laboratory for the Structure and Evolution of Celestial Objects, Chinese Academy of Sciences, Kunming 650216, China

[3] University of Chinese Academy of Sciences, Beijing 100049, China

Received 2017 October 27; accepted 2018 February 8

Abstract Type Ia supernovae (SNe Ia) are believed to be thermonuclear explosions of carbon oxygen (CO) white dwarfs (WDs) with masses close to the Chandrasekhar mass limit. How a CO WD accretes matter and grows in mass to this limit is not well understood, hindering our understanding of SN Ia explosions and the reliability of using SNe Ia as a cosmological distance indicator. In this work, we employed the stellar evolution code MESA to simulate the accretion process of hydrogen-rich material onto a $1.0\,M_{\odot}$ CO WD at a high rate (over the Eddington limit) of $4.3\times10^{-7}\,M_{\odot}\,\mathrm{yr}^{-1}$. The simulation demonstrates the characteristics of the double shell burning on top of the WD, with a hydrogen shell burning on top of a helium burning shell. The results show that helium shell burning is not steady (i.e. it flashes). Flashes from the helium shell are weaker than those in the case of accretion of helium-rich material onto a CO WD. The carbon to oxygen mass ratio resulting from the helium shell burning is higher than what was previously thought. Interestingly, the CO WD growing due to accretion has an outer part containing a small fraction of helium in addition to carbon and oxygen. The flashes become weaker and weaker as the accretion continues.

Key words: stars: evolution — supernovae: general — white dwarfs

1 INTRODUCTION

Type Ia supernovae (SNe Ia) play an important role in astrophysics. They have been successfully used as a cosmological distance indicator because of their high luminosity and remarkable uniformity. With SNe Ia, the expansion of the universe has been found to be accelerating, implying the existence of dark energy (Riess et al. 1998; Perlmutter et al. 1999). SNe Ia are also important for the chemical evolution of their host galaxies as iron-peak elements are mainly produced by SNe Ia (Helder et al. 2009; Howell 2011).

It is widely believed that SNe Ia are from the thermonuclear explosions of carbon-oxygen white dwarfs (CO WDs) (Hoyle & Fowler 1960). In the standard picture, a CO WD grows in mass somehow to $\sim$1.378 $M_{\odot}$, close to the Chandrasekhar mass limit and then explodes as an SN Ia (Nomoto et al. 1984). However, the exact nature of its progenitor is still unclear. Recently a lot of progenitor models of SNe Ia have been put forward (for a review, see Wang & Han 2012), and the favorite progenitor models are the single-degenerate (SD) model and the double-degenerate (DD) model. For the SD model, a non-degenerate star transfers mass to a CO WD in a binary system and the CO WD accretes the transferred material and grows in mass till it explodes (Whelan & Iben 1973; Nomoto et al. 1984; Hachisu et al. 1996; Han & Podsiadlowski 2004; Meng et al. 2009; Hillman et al. 2016; Meng & Podsiadlowski 2017). For the DD model, double white dwarfs (WDs) are brought together and coalesce due to angular momentum loss via gravitational wave radiation, and the merger is assumed to explode if the total mass is larger than the Chandrasekhar mass limit (Sparks & Stecher 1974; Iben & Tutukov 1984; Webbink 1984; Han 1998; Chen et al. 2012). Note, however, that

the merger of double WDs may lead to an accretion-induced-collapse, resulting in the formation of a neutron star rather than an SN Ia explosion, though recent simulations show that an SN Ia explosion is possible if the merger is violent (Pakmor et al. 2012). We mainly focus on the SD model in this study.

The mass growing process of a CO WD during its accretion is crucial for the SD model, and the mass growing process is mainly determined by the accretion rate. The accreted material burns steadily only for a narrow range of accretion rates. If the accretion rate is too low, the accreted material does not burn steadily and flashes. If the accretion rate is too high, the WD may evolve into a red-giant-type star due to the accumulation of accreted material. Hachisu et al. (1996) found an optically thick wind solution in the case of high accretion rate. In this scenario, the accreted material burns steadily at a critical rate while the unprocessed material is blown away by an optically thick wind. Recently, Ma et al. (2013) simulated the accretion of hydrogen-rich (H-rich) material onto CO WDs using the state-of-the-art stellar evolution code MESA, and found that a super-Eddington wind may be triggered at a much lower accretion rate than what was previously thought when the contribution of nuclear burning energy to the total luminosity is included. Wang et al. (2015) did a similar study, but for the accretion of helium-rich (He-rich) material onto CO WDs. They found that if the contribution of nuclear burning energy to the total luminosity is included when determining the Eddington accretion rate, a super-Eddington wind may also be triggered at an accretion rate significantly lower than that in previous studies based on steady-state models.

In previous studies on the accretion onto a CO WD, only hydrogen shell burning or helium shell burning is considered. However, the accretion is more complicated and usually leads to double shell burning. H-rich material is accreted onto a CO WD and the resulting hydrogen burning shell converts hydrogen to helium. The resulting helium shell underneath the hydrogen shell burns helium into carbon and oxygen, leading to the growth of the CO WD. The two shells may influence each other and the helium accretion rate is constrained by the hydrogen shell burning. Therefore, the helium accretion rate cannot span a very wide range as in those studies of accreting He-rich matter onto WDs (Kato & Hachisu 1999; Yoon & Langer 2003; Kato & Hachisu 2004; Wang et al. 2009a,b; Hillman et al. 2016).

In this paper, we study the accretion of H-rich material onto a CO WD and the resulting double shell burning. We use the state-of-the-art stellar evolution code MESA for simulating the accretion and double shell burning. The super-Eddington wind assumption of Ma et al. (2013) is adopted and the Eddington accretion rate is estimated by including the nuclear energy, gravothermal energy and radiation of the core in a way similar to that of Ma et al. (2013). The numerical code and basic methods are described in Section 2, and the simulation results are shown in Section 3. We discuss in Section 4 and conclude in Section 5.

2 THE SIMULATIONS

We employ the stellar evolution code MESA (Paxton et al. 2011, 2013, 2015) to simulate the accretion of H-rich material (with $X = 0.70, Y = 0.28, Z = 0.02$) onto a CO WD and consequently the double shell burning. We use the default opacity and equation of state tables (see figs. 1–2 in Paxton et al. 2011). The nuclear network consists of 21 isotopes (i.e., ^{1}H, ^{3}He, ^{4}He, ^{12}C, ^{13}C, ^{13}N, ^{14}N, ^{15}N, ^{14}O, ^{15}O, ^{16}O, ^{17}O, ^{18}O, ^{17}F, ^{18}F, ^{19}F, ^{18}Ne, ^{19}Ne, ^{20}Ne, ^{22}Mg and ^{24}Mg), which are coupled by 62 nuclear reactions.

Two relevant MESA suite cases are adopted for our simulations, i.e., make_co_wd and wd2. We use the suite case make_co_wd to create initial CO WD models, and then follow the accretion and double shell burning using the suite case wd2.

If the mass accretion rate is high enough, the luminosity L of the accreting WD may exceed the Eddington luminosity. The Eddington luminosity is defined as

$$L_{\rm Edd} = \frac{4\pi c G M_{\rm WD}}{\kappa}, \quad (1)$$

where c is the vacuum speed of light, G is the gravitational constant, M the WD mass and κ the opacity. Here, κ is the average opacity weighted by mass of outer layers of the accreting WD.[1] If L is larger than $L_{\rm Edd}$, a super-Eddington wind may be triggered, and the wind may blow away part of the accreted material at the surface of the WD.

The total luminosity L consists of four parts, i.e., the nuclear burning energy, gravothermal energy released by compression during accretion, thermal radiation of the core and gravitational energy released by the accreted material. Different from Ma et al. (2013), the helium

[1] Ma et al. (2013) used the opacity of the outermost layer, which is the default setting in the old version of MESA.

burning also contributes to the total luminosity. The details of these four parts of luminosity have been presented in Ma et al. (2013) and Wang et al. (2015). Here we follow the work of Ma et al. (2013), and adopt $\dot{M}_{\rm Edd}$ and $\dot{M}_{\rm stable}$ formulated by Ma et al. (2013) for H-shell burning, where $\dot{M}_{\rm Edd}$ is the Eddington accretion rate corresponding to the Eddington luminosity, and $\dot{M}_{\rm stable}$ the minimum accretion rate required for stable hydrogen shell burning. In this paper, we also follow helium burning, and we are therefore able to study the accretion of a CO WD more realistically, in particular we can monitor the hydrogen shell burning and the helium shell burning simultaneously.

Ma et al. (2013) identified the region of steady hydrogen shell burning for accretion of H-rich material onto CO WDs, while Wang et al. (2015) located the region similarly, but of steady helium shell burning for accretion of He-rich material onto CO WDs. We see that the accretion rate for the region of steady hydrogen shell burning is significantly lower than that of steady helium shell burning. The difference in accretion rates between the two regions is similar to that found in other studies (e.g. Piersanti et al. 2014). During the accretion of H-rich material, stable hydrogen shell burning converts hydrogen into helium, and consequently the helium accumulation rate is the same as that of the accretion rate of H-rich material. This seems to indicate that a helium shell underneath a stable hydrogen burning shell cannot burn steadily during the accretion of CO WDs.

In this paper, we evolve a $1.0\,M_{\odot}$ CO WD accreting H-rich material at a high accretion rate of $4.3 \times 10^{-7}\ M_{\odot}\ {\rm yr}^{-1}$, which is over the Eddington rate given by Ma et al. (2013), and then follow the resulting burning of the helium shell underneath the hydrogen burning shell. We then see how the helium shell burning is different from that in previous studies for the case of accretion of He-rich material without a hydrogen burning shell on top.

3 RESULTS

By adopting the Eddington accretion rate of Ma et al. (2013) for the accretion of H-rich material, we have followed the detailed evolution of an accreting CO WD with a mass of $1.0\,M_{\odot}$ and an accretion rate of $4.3 \times 10^{-7}\,M_{\odot}\,{\rm yr}^{-1}$, which is over the Eddington rate. The simulation results are displayed in Figures 1–6.

Figure 1 shows the luminosity evolution during the accretion. We see that the hydrogen shell burns steadily, but the helium shell does not. It is obvious that the accumulation rate of helium does not reach the rate for steady helium shell burning, and helium shell flashes occur.

Figure 2 exhibits the change of mass for the CO material of the accreting WD during accretion. We see that the mass of CO material on the WD keeps increasing though the helium shell does not burn steadily and flashes. This indicates that some of the CO material produced from helium shell flashes remains on top of the WD though some may have been blown away due to helium flashes.

Figure 3 plots profiles of the mass fractions of hydrogen, helium, carbon and oxygen in the inner core before flash cycle 8 (point A) in Figure 1. We see that the mass fraction of carbon resulting from helium shell flashes is quite different from that in the inner WD, and helium shell flashes result in higher carbon mass fraction. Furthermore, the flashes also lead to complex profile patterns visible in panel (b) of Figure 3.

To understand patterns of the chemical profiles, we have plotted how the profiles change during a flash in Figure 4. Figure 4 shows the profiles before a flash (point A), during the flash (point B with the maximum helium burning luminosity) and after the flash (point C) for the 8th helium flash cycle. We see that the flash leads to the formation of a spike in the profiles. We also notice that the helium flash does not burn all the helium and some helium remains. This means that the outer part of a CO WD which grows due to accretion may have helium, not just carbon, oxygen and metals.

Recently Hillman et al. (2016) simulated accretion of both H-rich material and He-rich material onto a CO WD. They found that although the amount of mass lost during the first few helium shell flashes is a significant fraction of that accumulated prior to the flashes, the fraction decreases with repeated helium shell flashes. Therefore, the helium flashes become gradually less violent and eventually settle down after a long term evolution. We adopt the peak nuclear-burning luminosity of a helium shell flash and the time interval between two adjacent helium shell flashes as indicators showing the strength of a helium flash.

Figure 5 displays the long term evolutionary calculation results in our study. The peak nuclear-burning luminosity decreases as a whole, while the flash time interval keeps reducing, which indicates that helium shell flashes become weaker and weaker during the accretion.

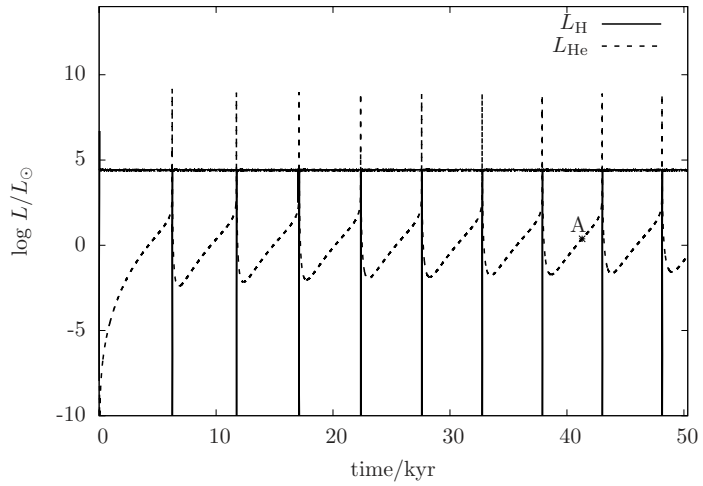

Fig. 1 Luminosity evolution for an accreting CO WD with a mass of 1.0 $M_\odot$ and an accretion rate of 4.3×10^{-7} $M_\odot$ yr^{-1}.

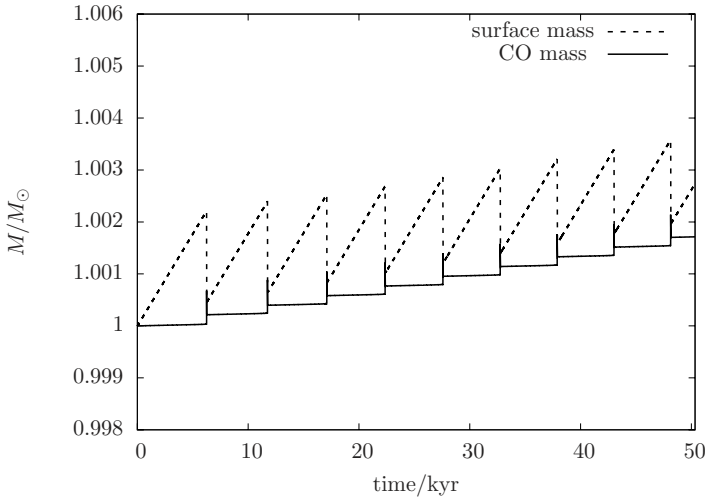

Fig. 2 Evolution of the surface mass and the mass of the CO material of the accreting WD.

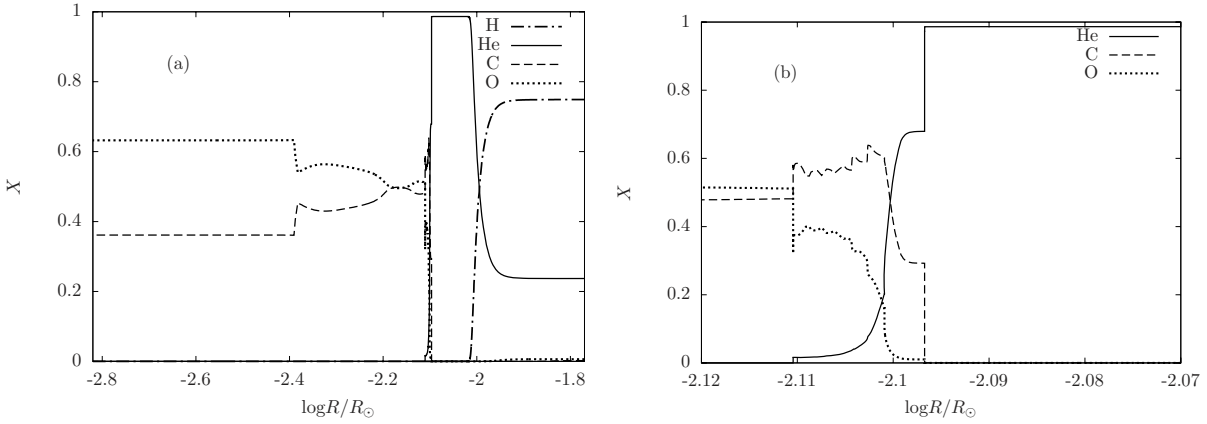

Fig. 3 The chemical profile of the accreting WD before flash cycle 8 (point A in Fig. 1) (panel a) and the part around $\log(R/R_\odot) = -2.1$ is enlarged (panel b).

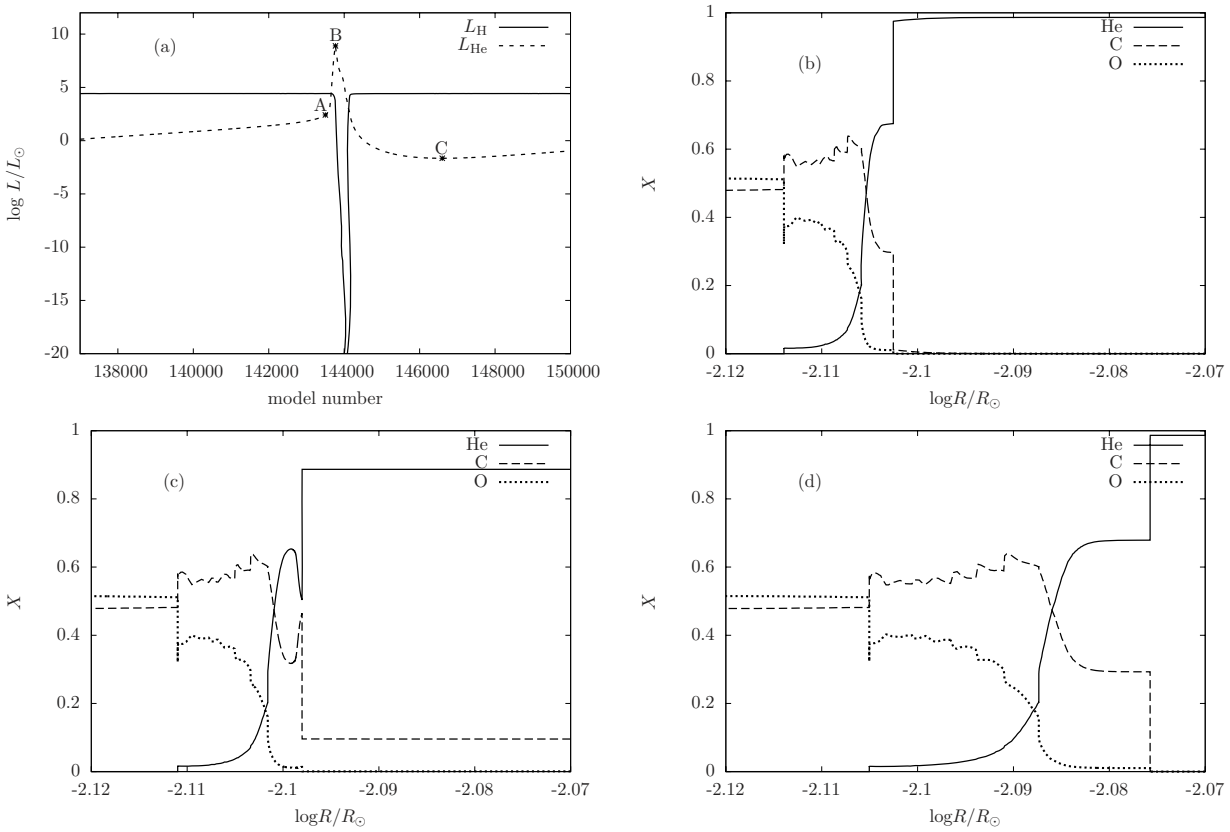

Fig. 4 Chemical profiles during the 8th He-shell flash cycle as in Fig. 1. Panel (a) shows the luminosity evolution of the cycle, while panels (b), (c) and (d) show the profiles at points A, B and C in panel (a), respectively.

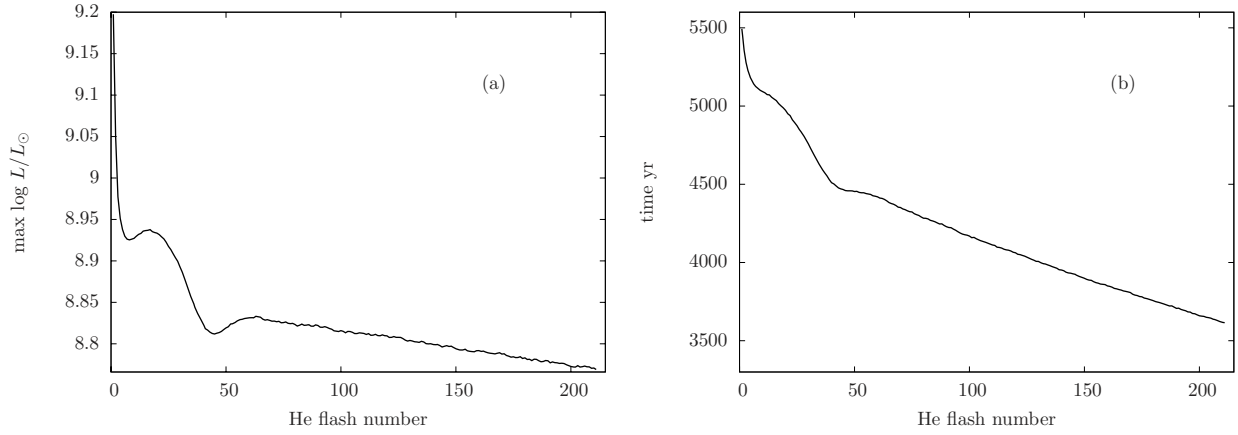

Fig. 5 The evolution of peak nuclear-burning luminosity for helium shell flashes (panel a) and the time interval between flashes (panel b).

4 DISCUSSION

In this paper, we have investigated the mass-growing process of a $1\,M_\odot$ CO WD accreting H-rich material. Different from Nomoto et al. (2007) and Ma et al. (2013), who just considered hydrogen shell burning, we also take helium shell burning into consideration in the simulation. We have followed the process of hydrogen shell burning and helium shell burning during the accretion, in which hydrogen shell burning converts hydrogen to

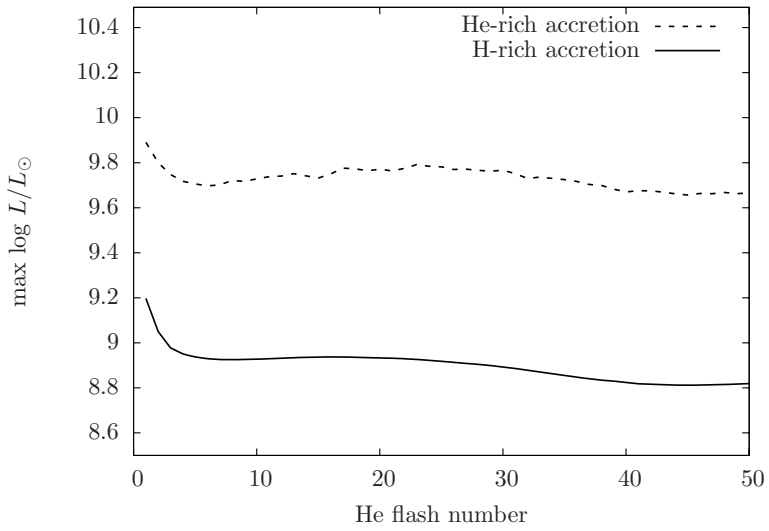

Fig. 6 The comparison of peak nuclear-burning luminosity of helium shell flashes for accretion of H-rich material onto a $1\,M_\odot$ CO WD with a helium accumulation rate of $3.5 \times 10^{-7}\,M_\odot\ \mathrm{yr}^{-1}$ and that for the He-rich material with the same rate for helium accretion.

helium and helium shell burning subsequently converts helium to carbon and oxygen, leading to growth of the CO WD.

In the simulation, the helium shell results from the hydrogen shell burning, and the accumulation rate of the helium shell depends on the burning rate of the hydrogen shell and thus on the accretion rate of H-rich material. The accretion rate of H-rich material is taken to be $4.3 \times 10^{-7}\,M_\odot \mathrm{yr}^{-1}$, which is over the Eddington accretion rate. As we have adopted the super-Eddington wind prescription of Ma et al. (2013), a super-Eddington wind is therefore assumed to be triggered for the accretion rate. Consequently, the accumulation rate of the helium shell is at its maximum ($\sim 3.5 \times 10^{-7}\,M_\odot\ \mathrm{yr}^{-1}$). We find that the He shell burning is not steady for the rate. This implies that a CO WD accreting H-rich material can only grow in mass via helium shell flashes, similar to what happens for low-rate accretion of He-rich material onto CO WDs (Kato & Hachisu 2004; Wang et al. 2015).

Wang et al. (2015) simulated the accretion of He-rich material onto WDs, and obtained the mass retention efficiency for helium shell flashes. To compare the strengths of helium shell flashes for accretion of H-rich material and that for accretion of He-rich material, in Figure 6 we plot the evolution of peak nuclear-burning luminosity of helium shell flashes for accretion of H-rich material onto a $1\,M_\odot$ CO WD with a helium accumulation rate of $3.5 \times 10^{-7}\,M_\odot\ \mathrm{yr}^{-1}$ and that for He-rich material with the same rate for helium accretion. We see that the peak luminosities for helium shell flashes are much lower for the case of accretion of the H-rich material. This indicates that the existence of a hydrogen-burning shell on top reduces the strength of helium shell flashes and consequently the mass retention efficiency is higher than for the accretion of He-rich material.

It is well known that calculations for helium shell flashes may be unreliable if the number of mass zones is too small. For our calculations, the number of mass zones is self adjusted. It is about 2000 to 2300 during the stable hydrogen-burning and about 2700 to 3000 during the helium shell flashes. In order to check whether or not the number of mass zones may affect our results, we manually vary the number of mass zones for some of our calculations and make a comparison in Figure 7. Panel (a) shows the chemical profiles for the same period during the calculations (after seven flash cycles), and the numbers of mass zones are set to be 2 times larger (short-dashed line) or 4 times larger (long-dashed line). The chemical profiles look almost the same for different numbers of mass zones. There is only a small difference in details for the carbon and oxygen profiles; this difference arises from increases in the number of mass zones and it does not change our conclusions. Panel (b) displays the evolution of peak nuclear-burning luminosity of helium shell flashes for different numbers of mass zones. It is clearly seen that the increase in number of mass zones practically does not affect our results.

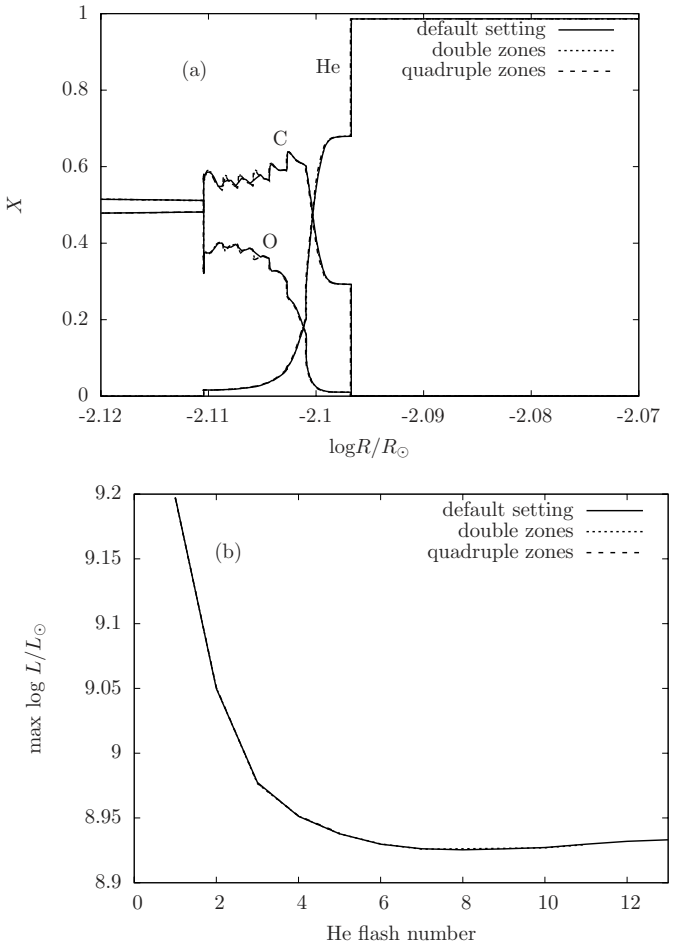

Fig. 7 The comparison of chemical profiles (panel a) and evolution of peak nuclear-burning luminosity of helium shell flashes (panel b) for different numbers of mass zones.

A higher ratio of carbon to oxygen (C/O) for a CO WD just before its explosion may make the resulting SN Ia more luminous (Umeda et al. 1999b,a; Höflich et al. 2010). Meng & Yang (2011) have investigated the C/O ratios of CO WDs at the moment of explosion. They followed the evolution of stars from zero-age main-sequence (ZAMS) to asymptotic giant branch (AGB). The AGB stars are assumed to lose their envelopes when their binding energy becomes positive (Han et al. 1994) and then evolve to CO WDs with C/O ratios resulting from central helium burning. It is the density and temperature of the helium burning region and later the mixing that determine the C/O ratio, and the C/O ratio resulting from central helium burning is low, around 0.25-0.5 (Umeda et al. 1999b). The CO WDs grow in mass due to accretion where a C/O ratio is simply assumed to be 1 by Meng & Yang (2011) for the shell burning due to accretion till the CO WDs reach the Chandrasekhar mass limit. We see from Figure 3 that C/O is about 1.5, higher than 1. Figure 3 also indicates that the chemical profiles of carbon and oxygen for the accreting WD are quite complicated.

5 CONCLUSIONS

Employing MESA, we have investigated the accretion of H-rich material onto a CO WD. We find that helium shell burning is not steady (i.e. there are helium shell burning flashes) even though hydrogen shell burning is steady enough (i.e. with a H-rich material accretion rate over the Eddington limit). However, the helium shell burning is more steady than that for accretion of He-rich material with the same helium accumulation rate. C/O ratio resulting from shell burning due to accretion is ~ 1.5 in the simulation, higher than previously believed. We have also noticed that not all the helium has been converted into carbon and oxygen during the double shell burning

and the outer part of the resulting CO WD has a small fraction of helium. As accretion continues, the flashes become weaker and weaker.

Acknowledgements We thank Xuefei Chen, Bo Wang, Hailiang Chen and Xin Ma for their helpful discussions and suggestions. This work is partly supported by the National Natural Science Foundation of China (Grant Nos. 11521303, 11733008, 11390374, 11473063, 11522327 and 11703081), the Natural Science Foundation of Yunnan Province (Grant Nos. 2013HA005, 2017HC018 and 2015HB096), CAS Light of West China Program and the Chinese Academy of Sciences (Grant No. KJZD-EW-M06-01).

References

Chen, X., Jeffery, C. S., Zhang, X., & Han, Z. 2012, ApJ, 755, L9
Hachisu, I., Kato, M., & Nomoto, K. 1996, ApJ, 470, L97
Han, Z. 1998, MNRAS, 296, 1019
Han, Z., Podsiadlowski, P., & Eggleton, P. P. 1994, MNRAS, 270, 121
Han, Z., & Podsiadlowski, P. 2004, MNRAS, 350, 1301
Helder, E. A., Vink, J., Bassa, C. G., et al. 2009, Science, 325, 719
Hillman, Y., Prialnik, D., Kovetz, A., & Shara, M. M. 2016, ApJ, 819, 168
Höflich, P., Krisciunas, K., Khokhlov, A. M., et al. 2010, ApJ, 710, 444
Howell, D. A. 2011, Nature Communications, 2, 350
Hoyle, F., & Fowler, W. A. 1960, ApJ, 132, 565
Iben, Jr., I., & Tutukov, A. V. 1984, ApJS, 54, 335
Kato, M., & Hachisu, I. 1999, ApJ, 513, L41
Kato, M., & Hachisu, I. 2004, ApJ, 613, L129
Ma, X., Chen, X., Chen, H.-l., Denissenkov, P. A., & Han, Z. 2013, ApJ, 778, L32
Meng, X. C., & Yang, W. M. 2011, A&A, 531, A94
Meng, X., Chen, X., & Han, Z. 2009, MNRAS, 395, 2103
Meng, X., & Podsiadlowski, P. 2017, MNRAS, 469, 4763
Nomoto, K., Thielemann, F.-K., & Yokoi, K. 1984, ApJ, 286, 644
Nomoto, K., Saio, H., Kato, M., & Hachisu, I. 2007, ApJ, 663, 1269
Pakmor, R., Kromer, M., Taubenberger, S., et al. 2012, ApJ, 747, L10
Paxton, B., Bildsten, L., Dotter, A., et al. 2011, ApJS, 192, 3
Paxton, B., Cantiello, M., Arras, P., et al. 2013, ApJS, 208, 4
Paxton, B., Marchant, P., Schwab, J., et al. 2015, ApJS, 220, 15
Perlmutter, S., Aldering, G., Goldhaber, G., et al. 1999, ApJ, 517, 565
Piersanti, L., Tornambé, A., & Yungelson, L. R. 2014, MNRAS, 445, 3239
Riess, A. G., Filippenko, A. V., Challis, P., et al. 1998, AJ, 116, 1009
Sparks, W. M., & Stecher, T. P. 1974, ApJ, 188, 149
Umeda, H., Nomoto, K., Kobayashi, C., Hachisu, I., & Kato, M. 1999a, ApJ, 522, L43
Umeda, H., Nomoto, K., Yamaoka, H., & Wanajo, S. 1999b, ApJ, 513, 861
Wang, B., Meng, X., Chen, X., & Han, Z. 2009a, MNRAS, 395, 847
Wang, B., Chen, X., Meng, X., & Han, Z. 2009b, ApJ, 701, 1540
Wang, B., & Han, Z. 2012, New Astron. Rev., 56, 122
Wang, B., Li, Y., Ma, X., et al. 2015, A&A, 584, A37
Webbink, R. F. 1984, ApJ, 277, 355
Whelan, J., & Iben, Jr., I. 1973, ApJ, 186, 1007
Yoon, S.-C., & Langer, N. 2003, A&A, 412, L53